

Novel Cyclohexylsilyl- or Phenylsilyl-Substituted Poly(*p*-phenylene vinylene)s via the Halogen Precursor Route and Gilch Polymerization

Taek Ahn, Seung-Won Ko, Jaemin Lee, and Hong-Ku Shim*

Center for Advanced Functional Polymers, Department of Chemistry and School of Molecular Science (BK 21), Korea Advanced Institute of Science and Technology, Taejeon 305-701, Korea

Received September 11, 2001; Revised Manuscript Received February 7, 2002

ABSTRACT: Novel cyclohexylsilyl- or phenylsilyl-substituted poly(1,4-phenylene vinylene) (PPV) derivatives, poly[2,5-bis(dimethylcyclohexylsilyl)-1,4-phenylene vinylene] (BDMCyS-PPV), poly[2,5-bis(dimethylphenylsilyl)-1,4-phenylene vinylene] (BDMPS-PPV), poly[2-dimethylcyclohexylsilyl-1,4-phenylene vinylene] (DMCyS-PPV), and poly[2-dimethylphenylsilyl-1,4-phenylene vinylene] (DMPS-PPV), were synthesized via the bromine precursor route (BPR) and Gilch dehydrohalogenation polyaddition. Thin films of the insoluble BDMCyS-PPV and BDMPS-PPV were fabricated from soluble polymer precursor materials by thermal conversion, and the electronic properties of these films were investigated. Monosilyl-substituted DMCyS-PPV and DMPS-PPV exhibited good solubility in the conjugated state, good film-forming properties, and high molecular weights. Moreover, they showed better thermal stability and higher values of T_g (DMCyS-PPV, 125 °C; DMPS-PPV, 127 °C) than other PPV derivatives including alkylsilyl-substituted PPVs; this improved mechanical stability led to good electroluminescence performance. Monocyclohexylsilyl- or phenylsilyl-substituted DMCyS-PPV and DMPS-PPV exhibited sharp PL emissions at about 511 and 513 nm, respectively, along with extremely high photoluminescence (PL) efficiencies in both solution and film (DMCyS-PPV, $\Phi_{\text{film}} = 0.83$; DMPS-PPV, $\Phi_{\text{film}} = 0.82$). LED devices fabricated from DMCyS-PPV and DMPS-PPV using the configuration ITO/polymer/Al showed electroluminescence (EL) maxima at 510 and 515 nm, respectively, with external EL quantum efficiencies of 0.02% and 0.03%. Incorporation of PVK as a hole-transporting layer between the ITO and polymer with an air-stable aluminum cathode caused a substantial improvement in the EL quantum efficiencies, increasing the values to 0.07% for DMCyS-PPV and 0.08% for DMPS-PPV.

Introduction

The discovery by the Cambridge group in 1990¹ that conjugated polymers can be used as active light-emitting layers in light-emitting devices triggered extensive research on this class of polymers.^{2–4} Polymeric light-emitting diodes (PLEDs) have many properties that are advantageous for the development of a large-area light-emitting displays: good processability, low operating voltages, fast response times, and color tunability over the full visible range by the control of the HOMO–LUMO band gap of the emissive layer.^{5–7} A number of conjugated backbone structures such as poly(*p*-phenylene vinylene) (PPV), poly(*p*-phenylene) (PPP),^{8,9} polythiophene (PT),¹⁰ and polyfluorene (PF)^{11–13} have been shown to be of importance in realizing a range of emissive colors from polymeric light-emitting diodes (PLEDs). The most promising and extensively studied group of polymers is poly(*p*-phenylene vinylene) (PPV) and its derivatives on account of their good device performance.¹⁴

There has been increasing interest in the silyl-substituted PPV derivatives as luminescent polymers since the first silicon-containing derivative, poly[2-(3-*epi*-cholestanol)-5-dimethylhexylsilyl-1,4-phenylene vinylene] (CS-PPV), was reported by Wudl et al.^{15,16} Silyl-substituted PPVs have many valuable properties such as high photoluminescence (PL) quantum efficiency, good solubility, and uniform film morphology. Holmes et al. demonstrated the high PL (ca. 60% in the film state) and electroluminescence (EL) (ca. 0.05% with Al

cathode) efficiencies of a PPV derivative with one octylsilyl substituent.^{17,18} Most recently, Huang et al. reported the synthesis of a family of bis-silyl-substituted PPVs with side-chain lengths ranging from C1 to C18.¹⁹ They found that the chemical/electrical stability and charge injection and transporting ability of the alkylsilyl-substituted polymers decreased with increasing chain length. In addition, they revealed that the introduction of silyl groups into PPVs retards the hole injection ability and that modification of the anode is the key factor in LED device performance. However, all the silyl-containing polymers synthesized to date have been composed of simple alkylsilyl-type side chains. Although such long alkylsilyl- or alkoxy-substituted PPV derivatives have good solubility in common organic solvents, they tend to have lower glass transition temperatures (T_g) than PPV.³ The low T_g in the PPV derivatives represent a drawback of the PPV precursor route. Tokito et al. found the operating lifetime of an EL device to be directly related to the T_g and thermal stability of the polymers used.²⁰ It is therefore important to synthesize silyl-substituted PPVs characterized by good mechanical properties (high T_g) and high solubility in order to obtain high PL efficiency and enhanced EL device performance.

Here we report the synthesis of bis (or mono)-cyclohexylsilyl- and phenylsilyl-substituted PPVs via the halogen precursor route^{21–23} and Gilch dehydrohalogenation^{14,24,25} method. Our results show that the cyclohexylsilyl- and phenylsilyl-substituted PPVs have enhanced thermal stabilities, mechanical properties, and PL and EL quantum efficiencies in comparison to the PPV derivatives prepared in the past.

* To whom correspondence should be addressed: Tel +82-42-869-2827; FAX +82-42-869-2810; e-mail hkshim@sorak.kaist.ac.kr.

Experimental Section

Materials. 2,5-Dibromo-*p*-xylene, 2-bromo-*p*-xylene, chlorodimethylcyclohexylsilane, chlorodimethylphenylsilane, *N*-bromosuccinimide (NBS), potassium *tert*-butoxide (1.0 M solution in THF), poly(9-vinylcarbazole) (PVK), and magnesium turnings from Aldrich Chemical Co. were used without further purification. Tetrahydrofuran (THF) was dried and fractionally distilled from sodium. All other solvents and reagents were analytical-grade quality, purchased commercially, and used without further purification.

Measurements. ^1H NMR and ^{13}C NMR spectra were recorded with the use of Bruker AVANCE 300 and 400 spectrometers, and chemical shifts were reported in ppm units with tetramethylsilane as an internal standard. Chloroform (CDCl_3) was mainly used as the solvent for recording NMR spectra. Melting points (mp) were determined using an Electrothermal model 1307 digital analyzer. Elemental analyses were performed by the Analytical Laboratory of Korea Advanced Institute of Science and Technology using an elemental analyzer (EA1110-FISONS). The FT-IR spectra were obtained by a Bruker EQUINOX 55 spectrometer by dispersing samples in KBr. Differential scanning calorimetry (DSC) and thermogravimetric analysis (TGA) were performed under nitrogen at a heating rate of $10\text{ }^\circ\text{C}/\text{min}$ with a DuPont 9900 analyzer. Cyclic voltammetry was performed on an AUTOLAB/PG-STAT12 model system with a three-electrode cell in a solution of Bu_4NBF_4 (0.10 M) in acetonitrile at a scan rate of 50 mV/s . Polymer films were coated on a square Pt electrode (0.50 cm^2) by dipping the electrode into the corresponding solutions and then drying in argon. A Pt wire was used as the counter electrode and a Ag/AgNO_3 (0.10 M in acetonitrile) electrode as the reference electrode. Gel permeation chromatography (GPC) analysis was conducted on a Waters GPC-150C model system using polystyrene as standard and THF as eluent. UV-vis spectra were measured on a Shimadzu UV-3100S spectrometer, and PL spectra of the polymers were obtained using a Spex Fluorolog-3 (model FL3-11) spectrofluorometer. Absorption and PL spectra were measured on polymer films spin-coated onto quartz substrates. The film thicknesses of the polymers were found by a Tencor Alpha-Step 500 surface profiler.

EL Device Fabrication. BDMCyS-PPV and BDMPS-PPV. Single-layer EL devices were fabricated with the polymer film sandwiched between an indium tin oxide (ITO) anode and an aluminum cathode. A glass substrate coated with transparent ITO was cleaned by successive ultrasonic treatment in isopropyl alcohol and acetone, then dried with nitrogen gas, and heated for further drying. Precursor polymer solutions (15 mg/mL in anhydrous chloroform) were spin-coated onto pre-cleaned ITO/glass substrates at a spin speed of 1500 rpm for 30 s. Thermal conversion of the precursor films was achieved by heating to $250\text{ }^\circ\text{C}$ in vacuo for 6 h. Aluminum electrodes (100 nm) were then evaporated on top of the polymer film below 2×10^{-6} Torr, yielding a circular active layer with a diameter of 2 mm.

DMCyS-PPV and DMPS-PPV. Single-layer and multi-layer LED devices were fabricated on glass substrates coated with indium tin oxide (ITO). The substrate was cleaned by the same method mentioned above prior to use. The hole-transporting layer of poly(9-vinylcarbazole) (PVK) (M_w 69 000 and M_n 27 200) was fabricated. PVK polymer solution (5 mg/mL in cyclohexanone) was spin-coated onto ITO/glass substrates at a spin speed of 3000 rpm for 30 s and baked at $100\text{ }^\circ\text{C}$ in vacuo for 1 h with the thickness of about 60 nm. The light-emitting layer (80 nm thick) of DMCyS-PPV or DMPS-PPV was spin-coated from chlorobenzene solutions (10 mg/mL) onto the ITO surface or the hole-transporting PVK layer. Light-emitting polymers coated on top of the PVK layer did not cause swelling or dissolution of the PVK layer, so good quality film interfaces were obtained. Finally, the Al cathode was vacuum-evaporated onto the light-emitting polymer layer as with the BDMCyS-PPV or BDMPS-PPV. For the enhanced LED device performance, a hole injection layer of poly(3,4-ethylenedioxythiophene) (PEDOT) doped with poly(sty-

renesulfonic acid) (PSS) (PEDOT:PSS) (BAYTRON P 4083) was prepared from water dispersion and baked at $100\text{ }^\circ\text{C}$ in vacuo for 1 h with a thickness of about 30 nm. PVK and DMPS-PPV layers were fabricated successively onto the PEDOT:PSS layer. The alkaline metal compound, LiF (2 nm), as an electron injection material (EIM) and Al (100 nm) cathode were vacuum-deposited onto the DMPS-PPV film at a pressure below 2×10^{-6} Torr, yielding an active area of 0.2 cm^2 . EL spectra of the LED device were measured with a Minolta CS-1000 spectroradiometer. Luminance-current-voltage (L - I - V) characteristics were recorded using a programmable current/voltage source (Keithley 238) and a luminance meter (Minolta LS-100).

2,5-Bis(dimethylcyclohexylsilyl)-*p*-xylene (1). To a solution of 10 g (38.0 mmol) of 2,5-dibromo-*p*-xylene diluted in anhydrous THF was added 3.7 g (152 mmol) of clean magnesium turnings after initiation by 5 mol % of dibromoethane, and then this solution was refluxed for 3 h under a nitrogen atmosphere. When a gray, soupy Grignard reagent was formed, 21.1 mL (114 mmol) of chlorodimethylcyclohexylsilane was slowly added to this solution, and the mixture was refluxed for 9 h. The reaction was quenched with dilute HCl solution. The organic layer was separated and washed with water several times. The solution was dried with magnesium sulfate, and then THF was removed by evaporation. A white, solid product was obtained by recrystallization from methanol. The product yield was 5.7 g (39%); mp 112 – $114\text{ }^\circ\text{C}$. ^1H NMR (CDCl_3 , ppm): δ 7.14 (s, 2H, Ar H), 2.38 (s, 6H, CH_3), 1.70–1.51 (m, 10H, CH and CH_2 of cyclohexyl), 1.25–0.93 (m, 12H, CH_2 of cyclohexyl), 0.24 (s, 12H, SiCH_3). ^{13}C NMR (CDCl_3 , ppm): δ 139.33, 137.36, 136.41, 28.22, 27.74, 26.99, 25.74, 23.01, –3.77. Anal. Calcd for $\text{C}_{24}\text{H}_{42}\text{Si}_2$: C, 74.53; H, 10.95. Found: C, 73.95; H, 11.26.

2,5-Bis(dimethylcyclohexylsilyl)-1,4-bis(bromomethyl)benzene (2). Compound **2** was prepared by reacting 3.0 g (7.76 mmol) of **1** with 2.9 g (16.3 mmol) of *N*-bromosuccinimide (NBS) in 80 mL of carbon tetrachloride (CCl_4). A small amount of benzoyl peroxide was added as an initiator. The reaction mixture was refluxed at $80\text{ }^\circ\text{C}$ for 3 h under nitrogen atmosphere. The completion of the reaction was indicated by the appearance of succinimide on the surface of the reaction solution. The organic layer was washed with water and brine and then dried over anhydrous magnesium sulfate. The solution was concentrated and poured into methanol. The pure white solid was obtained by recrystallizing the resulting precipitate from methanol. The product yield was 2.8 g (66%); mp 94 – $96\text{ }^\circ\text{C}$. ^1H NMR (CDCl_3 , ppm): δ 7.45 (s, 2H, Ar H), 4.60 (s, 4H, CH_2Br), 1.70–1.52 (m, 10H, CH and CH_2 of cyclohexyl), 1.24–1.06 (m, 12H, CH_2 of cyclohexyl), 0.32 (s, 12H, SiCH_3). ^{13}C NMR (CDCl_3 , ppm): δ 142.01, 139.06, 138.11, 34.48, 27.99, 27.57, 26.83, 26.02, –3.58. Anal. Calcd for $\text{C}_{24}\text{H}_{40}\text{Br}_2\text{Si}_2$: C, 52.93; H, 7.40. Found: C, 52.13; H, 8.05.

2,5-Bis(dimethylphenylsilyl)-*p*-xylene (3). To a solution of 10 g (38.0 mmol) of 2,5-dibromo-*p*-xylene diluted in anhydrous THF was added 3.7 g (152 mmol) of clean magnesium turnings after initiation by 5 mol % of dibromoethane, and then this solution was refluxed for 3 h under a nitrogen atmosphere. When a gray, soupy Grignard reagent was formed, 19.1 mL (114 mmol) of chlorodimethylphenylsilane was slowly added to this solution, and the mixture was refluxed for 9 h. The following synthetic procedures were performed in analogy to the procedures given for compound **1**. The product yield was 6.8 g (48%); mp 121 – $123\text{ }^\circ\text{C}$. ^1H NMR (CDCl_3 , ppm): δ 7.52 (m, 4H, Ar H), 7.35 (m, 6H, Ar H), 7.25 (m, 2H, Ar H), 2.46 (s, 6H, CH_3), 0.59 (s, 12H, SiCH_3). ^{13}C NMR (CDCl_3 , ppm): δ 140.03, 138.97, 137.38, 136.72, 134.04, 128.90, 127.80, 22.77, –1.38. Anal. Calcd for $\text{C}_{24}\text{H}_{30}\text{Si}_2$: C, 76.94; H, 8.07. Found: C, 76.66; H, 8.01.

2,5-Bis(dimethylphenylsilyl)-1,4-bis(bromomethyl)benzene (4). Compound **4** was prepared by reacting 5.0 g (13.4 mmol) of **3** with 4.9 g (28 mmol) of *N*-bromosuccinimide (NBS) in 100 mL of carbon tetrachloride (CCl_4). The following synthetic procedures were performed in analogy to the procedures given for compound **2**. The product yield was 5.1 g (72%); mp 199 – $121\text{ }^\circ\text{C}$. ^1H NMR (CDCl_3 , ppm): δ 7.57 (s, 2H, Ar H),

7.52 (m, 4H, Ar H), 7.36 (m, 6H, Ar H), 4.41 (s, 4H, CH₂Br), 0.66 (s, 12H, SiCH₃). ¹³C NMR (CDCl₃, ppm): δ 142.54, 139.21, 138.40, 137.86, 133.98, 129.44, 128.07, 34.00, -1.10. Anal. Calcd for C₂₄H₂₈Br₂Si₂: C, 54.14; H, 5.30. Found: C, 53.99; H, 5.89.

2-Dimethylcyclohexylsilyl-*p*-xylene (5). To a solution of 2-bromo-*p*-xylene (10 g, 54.0 mmol) in anhydrous THF was slowly added clean magnesium turnings (2.27 g, 93.5 mmol) after initiation by 5 mol % of 1,2-dibromoethane at 80 °C. When the magnesium turnings were completely consumed, chlorodimethylcyclohexylsilane (13.4 mL, 71.5 mmol) was added. The mixture was heated to reflux for 6 h, and the reaction was quenched with dilute aqueous HCl solution. The THF layer was separated and washed with water several times, and the solvent was removed on the rotary evaporator. The residue was vacuum-distilled to give a colorless liquid product. The yield was 5.2 g (38%). ¹H NMR (CDCl₃, ppm): δ 7.23 (m, 1H, Ar H), 7.06 (m, 2H, Ar H), 2.4 (s, 3H, CH₃), 2.3 (s, 3H, CH₃), 1.72–1.61 (m, 5H, CH and CH₂ of cyclohexyl), 1.28–1.08 (m, 6H, CH₂ of cyclohexyl), 0.28 (s, 6H, SiCH₃). ¹³C NMR (CDCl₃, ppm): δ 140.43, 136.60, 135.79, 133.72, 129.66, 128.89, 28.19, 27.71, 26.95, 25.72, 22.84, 21.10, -3.75. Anal. Calcd for C₁₆H₂₆Si: C, 77.97; H, 10.63. Found: C, 77.23; H, 9.89.

2-Dimethylcyclohexylsilyl-1,4-bis(bromomethyl)benzene (6). To a solution of 2-dimethylcyclohexylsilyl-*p*-xylene (7.0 g, 28.4 mmol) in carbon tetrachloride (80 mL) was added *N*-bromosuccinimide (10.7 g, 59.6 mmol) and benzoyl peroxide as an initiator. The reaction mixture was heated to reflux at 80 °C for 4 h under a nitrogen atmosphere. The completion of the reaction was indicated by the appearance of succinimide on the surface of the reaction solution. The organic layer was washed with water and brine and then dried over anhydrous magnesium sulfate. After evaporation of the solvent, a yellowish oil was obtained. Chromatography on a silica column using hexane as eluent gave the brominated product as a colorless oil. The product yield was 5.4 g (47%). ¹H NMR (CDCl₃, ppm): δ 7.42–7.24 (m, 2H, Ar H), 7.26–7.22 (m, 1H, Ar H), 4.58 (s, 2H, CH₂Br), 4.47 (s, 2H, CH₂Br), 1.71–1.59 (m, 5H, CH and CH₂ of cyclohexyl), 1.27–0.90 (m, 6H, CH₂ of cyclohexyl), 0.34 (s, 6H, SiCH₃). ¹³C NMR (CDCl₃, ppm): δ 143.41, 138.36, 136.70, 135.84, 132.07, 130.22, 41.44, 40.41, 28.11, 27.50, 27.31, 14.11, -4.11. Anal. Calcd for C₁₆H₂₄Br₂Si: C, 47.54; H, 5.98. Found: C, 47.88; H, 5.78.

2-Dimethylphenylsilyl-*p*-xylene (7). To a solution of 2-bromo-*p*-xylene (10.0 g, 54.0 mmol) in anhydrous THF was slowly added clean magnesium turnings (2.23 g, 92.0 mmol) after initiation by 5 mol % of 1,2-dibromoethane at 80 °C. When the magnesium turnings were completely consumed, chlorodimethylphenylsilane (15.4 mL, 92.0 mmol) was added. The following synthetic procedures were performed in analogy to the procedures given for compound 5. The yield was 6.2 g (48%). ¹H NMR (CDCl₃, ppm): δ 7.52 (m, 2H, Ar H), 7.36 (m, 4H, Ar H), 7.14 (d, 1H, Ar H), 7.08 (d, 1H, Ar H), 2.35 (s, 3H, CH₃), 2.24 (s, 3H, CH₃), 0.60 (s, 6H, SiCH₃). ¹³C NMR (CDCl₃): δ 140.90, 139.05, 135.99, 135.80, 133.94, 133.53, 130.28, 129.83, 128.83, 127.76, 22.60, 21.08, -1.36. Anal. Calcd for C₁₆H₂₀Si: C, 79.93; H, 8.38. Found: C, 78.80; H, 8.09.

2-Dimethylphenylsilyl-1,4-bis(bromomethyl)benzene (8). To a solution of 2-dimethylphenylsilyl-*p*-xylene (7.0 g, 29.0 mmol) in carbon tetrachloride (100 mL) was added *N*-bromosuccinimide (11.5 g, 64.0 mmol) and benzoyl peroxide as an initiator. The following synthetic procedures were performed in analogy to the procedures given for compound 6. The product yield was 6.0 g (52%). ¹H NMR (CDCl₃, ppm): δ 7.51–7.42 (m, 5H, Ar H), 7.38–7.24 (m, 3H, Ar H), 4.46 (s, 2H, CH₂Br), 4.36 (s, 2H, CH₂Br), 0.64 (s, 6H, SiCH₃). ¹³C NMR (CDCl₃, ppm): δ 143.82, 137.76, 136.95, 133.93, 131.68, 130.87, 129.79, 129.45, 128.85, 128.16, 33.62, 33.14, -1.05. Anal. Calcd for C₁₆H₁₈Br₂Si: C, 48.26; H, 4.56. Found: C, 47.88; H, 4.78.

Polymerization. Poly[**2,5-bis(dimethylcyclohexylsilyl)-1,4-phenylene**]{**1-bromoethylene**}-*co*-[**2,5-bis(dimethylcyclohexylsilyl)-1,4-phenylene vinylene**]} (**9**). A solution of potassium *tert*-butoxide (87 mg, 0.73 mmol) dissolved in dry tetrahydrofuran (3 mL) was added to a stirred solution of 2,5-

bis(dimethylcyclohexylsilyl)-1,4-bis(bromomethyl)benzene (**2**) (0.5 g, 0.92 mmol) in dry tetrahydrofuran (3 mL), which was cooled with an acetone/ice bath under nitrogen. A viscous sky-blue solution was formed. The reaction mixture was allowed to warm to room temperature after 10 min and stirred for 2 h. Polymer **9** was precipitated by adding the reaction mixture dropwise to ice-cooled methanol (30 mL). The mixture was filtered, and the residue, polymer **9**, was briefly dried under vacuum. The residue was dissolved in dry chloroform, and the polymer was precipitated again by addition to an excess methanol. The mixture was filtered, and the residue was collected. The procedure was repeated twice more to yield a sky-blue solid of **9**. The polymer yield was 49% (0.21 g). ¹H NMR (CDCl₃, ppm): δ 8.10–7.81 (br m, vinyl H), 7.45–6.61 (br m, Ar H and vinyl H), 5.65–5.15 (br m, CHBr), 3.97–2.96 (br m, ArCH₂), 2.75–0.80 (br m, CH and CH₂ of cyclohexyl), 0.79 to -0.60 (br m, -Si(CH₃)₂).

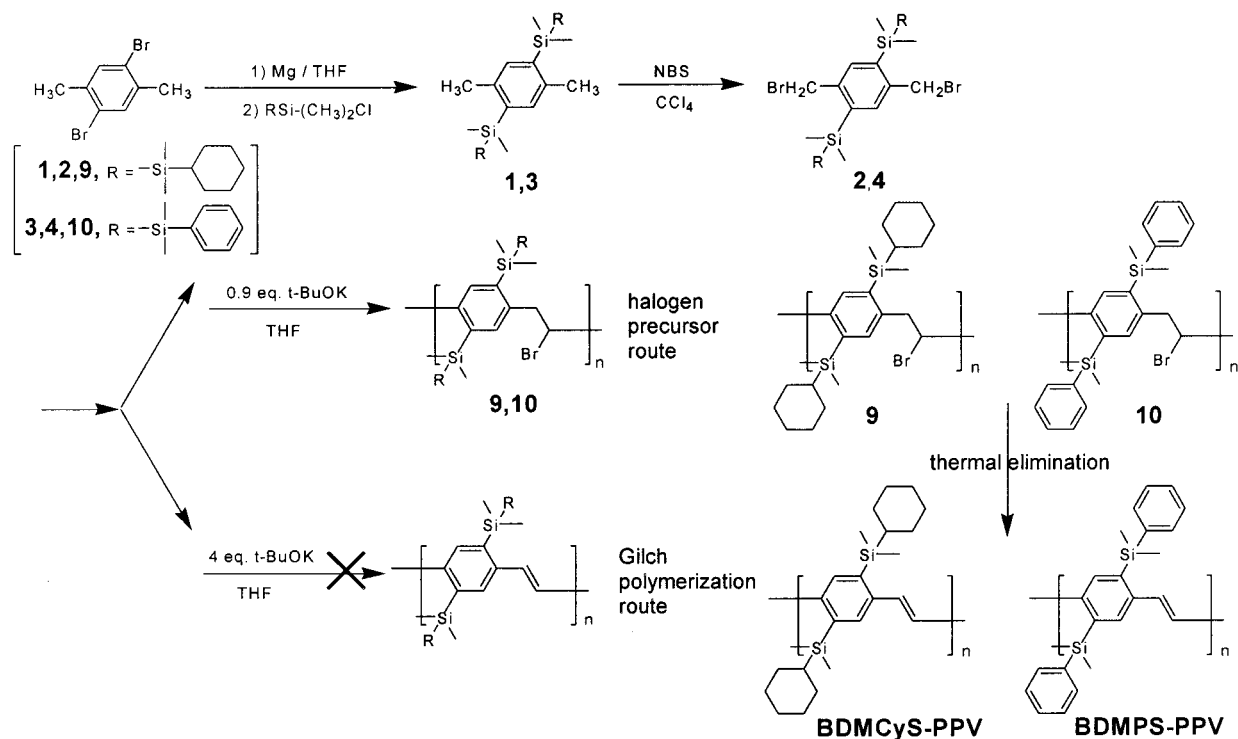
Poly[2,5-bis(dimethylphenylsilyl)-1,4-phenylene**]{**1-bromoethylene**}-*co*-[**2,5-bis(dimethylphenylsilyl)-1,4-phenylenevinylene**]} (**10**). A solution of potassium *tert*-butoxide (89 mg, 0.75 mmol) dissolved in dry tetrahydrofuran (3 mL) was added to a stirred solution of 2,5-bis(dimethylphenylsilyl)-1,4-bis(bromomethyl)benzene (**4**) (0.5 g, 0.94 mmol) in dry tetrahydrofuran (3 mL), which was cooled with an acetone/ice bath under nitrogen. A viscous sky-blue solution was formed. The following synthetic procedures were performed in analogy to the procedures given for precursor polymer **9**. The polymer yield was 55% (0.23 g). ¹H NMR (CDCl₃, ppm): δ 7.77–7.59 (br m, vinyl H), 7.39–6.63 (br m, Ar H and vinyl H), 5.25–5.01 (br m, CHBr), 3.47–2.66 (br m, ArCH₂), 1.02 to -0.15 (br m -Si(CH₃)₂).**

Poly[2-(dimethylcyclohexylsilyl)-1,4-phenylene**]{**1-bromoethylene**}-*co*-[**2-(dimethylcyclohexylsilyl)-1,4-phenylene vinylene**]} (**11**). A solution of potassium *tert*-butoxide (131 mg, 1.10 mmol) dissolved in dry tetrahydrofuran (3 mL) was added to a stirred solution of 2-dimethylcyclohexylsilyl-1,4-bis(bromomethyl)benzene (**6**) (0.5 g, 1.23 mmol) in dry tetrahydrofuran (3 mL) cooled with an acetone/ice bath under nitrogen. A viscous sky-blue solution was formed. The following synthetic procedures were performed in analogy to the procedures given for precursor polymer **9**. The polymer yield was 45% (0.18 g). ¹H NMR (CDCl₃, ppm): δ 7.79–6.65 (br m, vinyl H and Ar H), 5.75–4.95 (br m, CHBr), 3.71–2.89 (br m, ArCH₂), 2.35–0.80 (br m, CH and CH₂ of cyclohexyl), 0.75 to -0.17 (br m, -Si(CH₃)₂).**

Poly[2-(dimethylphenylsilyl)-1,4-phenylene**]{**1-bromoethylene**}-*co*-[**2-dimethylphenylsilyl)-1,4-phenylene vinylene**]} (**12**). A solution of potassium *tert*-butoxide (134 mg, 1.13 mmol) dissolved in dry tetrahydrofuran (3 mL) was added to a stirred solution of 2-dimethylphenylsilyl-1,4-bis(bromomethyl)benzene (**8**) (0.5 g, 1.26 mmol) in dry tetrahydrofuran (3 mL) cooled with an acetone/ice bath under nitrogen. A viscous sky-blue solution was formed. The following synthetic procedures were performed in analogy to the procedures given for precursor polymer **9**. The polymer yield was 50% (0.20 g). ¹H NMR (CDCl₃, ppm): δ 7.67–6.69 (br m, ArH and vinyl H), 6.12–5.75, 5.65–5.32, 5.25–4.85, 4.84–4.61 (br m, CHBr), 3.67–2.86 (br m, ArCH₂), 0.89–0.25 (br m -Si(CH₃)₂).**

Poly[2-dimethylcyclohexylsilyl-1,4-phenylene vinylene**]** (**DMCyS-PPV**). The monomer **6** (0.5 g 1.23 mmol) was dissolved in 30 mL of THF with 29 mg (0.123 mmol) of *tert*-butylbenzyl bromide as an end-capper, and then the solution was cooled to 0 °C. The initiator, 3.69 mL (3.69 mmol) of potassium *tert*-butoxide (1.0 M in THF), was added to the solution. The reaction mixture became progressively green and viscous during the addition. The highly viscous solution was stirred at 0 °C for 3 h. The polymerization reaction was poured into 300 mL of methanol with vigorous stirring. The resulting yellow precipitate was collected, dissolved in chloroform, and reprecipitated in methanol/acetone (1/1) cosolvent twice more. The polymer was extracted with a Soxhlet extractor from methanol for 24 h and dried under vacuum. The polymer yield was 57% (0.17 g) of a yellow fiber type. FT-IR (KBr) ν_{max}/cm⁻¹: 3059, 2924, 2845, 1489, 1449, 1252, 1142, 1102, 1070, 1000,

Scheme 1. Synthetic Route for BDMCyS-PPV and BDMPS-PPV



960, 889, 842, 802, 763, 645. ¹H NMR (CDCl₃, ppm): δ 7.88–6.80 (br m, 5H, Ar H and vinylic H), 1.98–1.33 (br s, 5H, CH and CH₂ of cyclohexyl), 1.31–0.78 (br s, 6H, CH₂ of cyclohexyl), 0.71–0.40 (br s, 6H, –Si(CH₃)₂). Anal. Calcd for (C₁₆H₂₂Si)_n: C, 79.25; H, 9.16. Found: C, 79.01; H, 9.78.

Poly[2-dimethylphenylsilyl-1,4-phenylene vinylene] (DMPS-PPV). The monomer **8** (0.5 g 1.26 mmol) was dissolved in 30 mL of THF with 30 mg (0.126 mmol) of *tert*-butylbenzyl bromide as an end-capper, and then the solution was cooled to 0 °C. The initiator, 3.78 mL (3.78 mmol) of potassium *tert*-butoxide (1.0 M in THF), was added to the solution. The reaction mixture became progressively green and viscous during the addition. The following synthetic procedures were performed in analogy to the procedures given for DMCyS-PPV. The polymer yield was 60% (0.18 g) of a yellow fiber type. FT-IR (KBr) ν_{\max} /cm⁻¹: 3074, 3043, 3011, 2956, 1481, 1426, 1252, 1110, 1063, 961, 905, 810, 771, 731, 692, 645, 582, 463. ¹H NMR (CDCl₃, ppm): δ 7.98–6.82 (br m, 10H, Ar H and vinylic H), 0.98–0.10 (br s, 6H, –Si(CH₃)₂). Anal. Calcd for (C₁₆H₁₆Si)_n: C, 81.28; H, 6.84. Found: C, 80.88; H, 6.78.

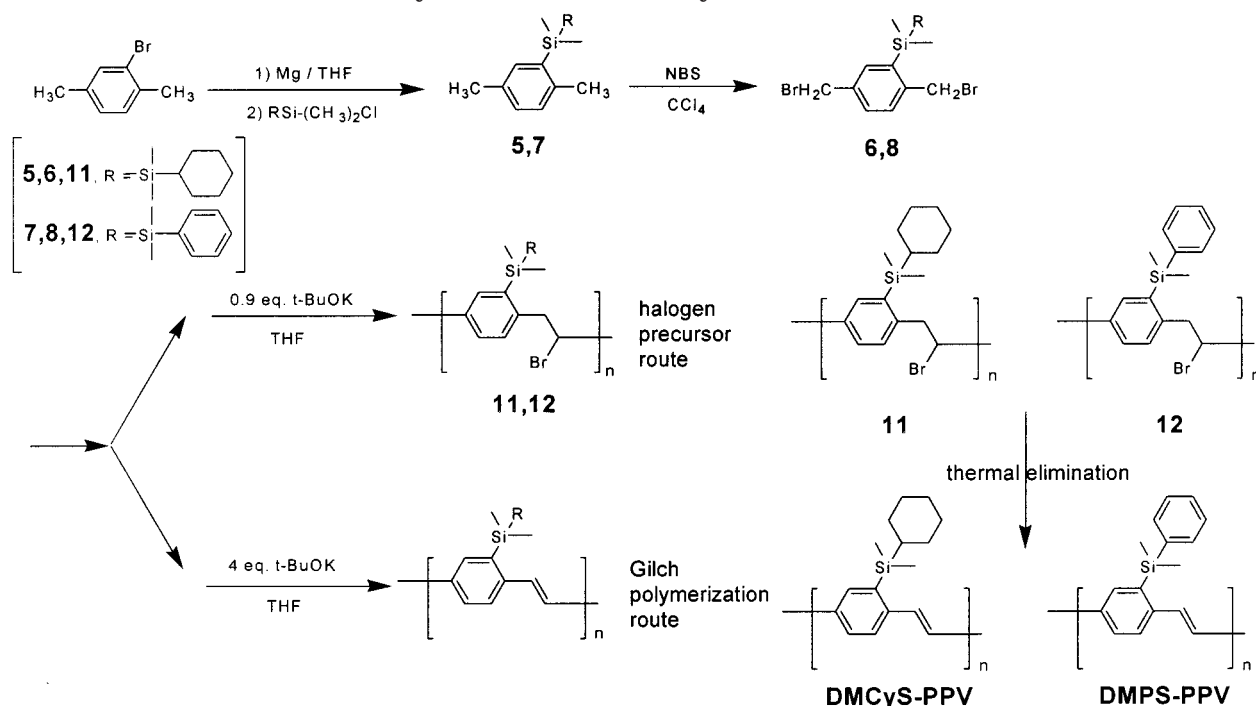
Poly[2-methoxy-5-(2-ethylhexyloxy)-1,4-phenylene vinylene] (MEH-PPV). The well-known MEH-PPV was synthesized by the method of dehydrohalogenation route (the Gilch procedure).^{26,27} The final polymer was soluble in common organic solvents.

Results and Discussion

Synthesis and Characterization. The synthetic routes used to prepare the mono (or bis)cyclohexylsilyl- or phenylsilyl-containing bis(bromomethyl)-type monomers, the resulting precursor polymers (halogen precursor route),^{21–23} and the soluble polymers (Gilch route)^{14,24,25} are presented in Schemes 1 and 2. We incorporated a dimethylcyclohexylsilyl or dimethylphenylsilyl group as a polymer side chain using the Grignard reaction. Each bis(bromomethyl) monomer was polymerized using two synthetic methods: the bromine precursor route (BPR) and Gilch polymerization. First, bis(silyl)-substituted **2** and **4** monomers were polymerized using excess base (Gilch route). However, this

method yielded polymer particles that were insoluble in common organic solvents. This result is in contrast to the case of bis(alkylsilyl)-substituted PPVs, which have been shown to have soluble final conjugated forms.¹⁹ The use of inflexible side chains causes bis(silyl)-substituted BDMCyS-PPV and BDMPS-PPV to have symmetric structures and therefore to show lower solubility. To circumvent the problem of the polymer solubility, we carried out the 1,6-polymerization and the 1,2-elimination separately. Using this method, a precursor polymer is first obtained which is then converted to the corresponding bis(silyl)-containing polymers. This precursor approach has been used extensively for the fabrication of insoluble PPV thin films from a soluble polymer precursor material.^{3,21} The bis(bromomethyl) monomers **2** and **4** were polymerized under the standard conditions to give the precursor polymers **9** and **10**, respectively. In each case, a solution of 0.9 equiv of potassium *tert*-butoxide in tetrahydrofuran was added to a solution of **2** or **4** in tetrahydrofuran cooled in an acetone/ice bath. The reaction mixtures were then allowed to warm to room temperature and stirred for 2 h. The precursor polymers **9** and **10** were purified by reprecipitation from chloroform using methanol. The monosilyl-containing monomers **6** and **8** were also synthesized via the BPR and Gilch polymerization routes. Monocyclohexylsilyl- or monophenylsilyl-substituted precursor polymers were obtained using polymerization conditions similar to those described above for the synthesis of the bis(silyl)-containing precursor polymers. In the case of the polymers containing monosilyl, most attention was focused on the direct polymerization into the final conjugated forms DMCyS-PPV and DMPS-PPV. The monomers containing monosilyl (**6** and **8**) were easily polymerized via the Gilch dehydrohalogenation route under ambient conditions using excess potassium *tert*-butoxide as the base in dry THF. Chloroform solutions of the polymers were precipitated

Scheme 2. Synthetic Route for DMCyS-PPV and DMPS-PPV



twice or more in methanol/acetone (1/1) cosolvent, yielding yellow solid products. The collected polymers were further purified by Soxhlet extraction through methanol. The two polymers synthesized by the Gilch route, DMCyS-PPV and DMPS-PPV, were completely soluble in common organic solvents such as chloroform, chlorobenzene, THF, 1,2-dichloroethane, and toluene. Huang et al. reported that silyl-substituted PPVs have few structural defects (bis(benzyl) and diphenylacetylene moieties, etc.) in their polymer chains and that the silyl groups contribute to the satisfactory solubility of these polymers because of the larger atomic size of Si compared to C and O as well as the longer bond length of Si-C compared to C-C and C-O.¹⁹

The molecular weights of the polymers were measured by gel permeation chromatography using THF as eluent and polystyrene as standard. The number-average molecular weights, M_n , of the monosilyl-substituted DMCyS-PPV and DMPS-PPV, obtained by the Gilch route, were 351 000 ($M_w/M_n = 4.1$) and 292 000 ($M_w/M_n = 3.9$), respectively, which are very high compared to those of the simple alkylsilyl-substituted PPVs prepared in the past. The four precursor polymers (**9**, **10**, **11**, and **12**) synthesized by the BPR method showed relatively low molecular weights compared with the polymers prepared by the Gilch route. The number-average molecular weight (M_n), weight-average molecular weight (M_w), and polydispersity index (PDI) results are summarized in Table 1. The ¹H NMR spectra of the synthesized polymers showed signal broadening, but the chemical shifts are consistent with the proposed polymer structures. The assignments for these spectra are documented in the Experimental Section. The signal at 7.24 ppm originates from the chloroform-*d* used as a solvent, and the peaks in the ranges 6–5 and 4–2.5 ppm observed for all precursor polymers are assigned to the protons in CHBr and ArCH₂, respectively.²² However, the conjugated DMCyS-PPV and DMPS-PPV polymers synthesized by the Gilch method show no peaks between 2.5 and 6 ppm. The polymers containing

Table 1. Polymerization Results and Thermal Properties of Polymers

polymer	yield (%)	M_n^a	M_w^a	PDI ^a	T_g (°C)	T_{ID}^b (°C)
9	49	9.8×10^4	2.5×10^5	2.56		168 ^c
10	55	1.1×10^5	2.8×10^5	2.59		163 ^c
11	45	7.3×10^4	5.9×10^5	8.10		179 ^c
12	50	7.2×10^4	6.3×10^5	8.70		164 ^c
DMCyS-PPV	57	3.5×10^5	1.4×10^6	4.10	125	428
DMPS-PPV	60	2.9×10^5	1.1×10^6	3.88	127	435

^a M_n , M_w , and PDI of the polymers were determined by gel permeation chromatography using polystyrene standards. ^b Temperature at which initial loss of mass (5%) was observed. ^c Mainly due to the loss of hydrogen bromide.

cyclohexylsilyl exhibit peaks in the region of 2–1 ppm, corresponding to the CH and CH₂ of the cyclohexyl. FT-IR spectra of the precursor polymers **11** and **12**, DMCyS-PPV and DMPS-PPV, are measured. The spectra of these polymers are very similar except for the additional peak at about 960 cm⁻¹ in the spectra of DMCyS-PPV and DMPS-PPV, which is attributed to the out-of-plane deformation of the trans C-H of the alkene moiety.^{7,23} This result suggests that the vinylene group formed through the Gilch route is in the trans configuration. In addition, all polymers showed the absorption band characteristic of Si-CH₃ at 1250 cm⁻¹, with a very sharp peak of strong intensity.¹⁹

Thermogravimetric analysis of the precursor polymers **9**–**12** showed a significant weight loss at approximately 160 °C due to the loss of hydrogen bromide.²³ DMCyS-PPV and DMPS-PPV from the Gilch route showed less than 5% weight loss on heating to about 400 °C. The 5% weight loss temperatures for DMCyS-PPV and DMPS-PPV were 428 and 435 °C, respectively. These polymers therefore show much higher thermal stability than those of the simple alkylsilyl-PPVs (the 5% weight loss temperatures for butylsilyl-PPV and decylsilyl-PPV are reported as 392 and 371 °C, respectively)¹⁹ (Figure 1). In addition to higher thermal stability, the cyclohexylsilyl- or phenylsilyl-substituted PPVs (DMCyS-

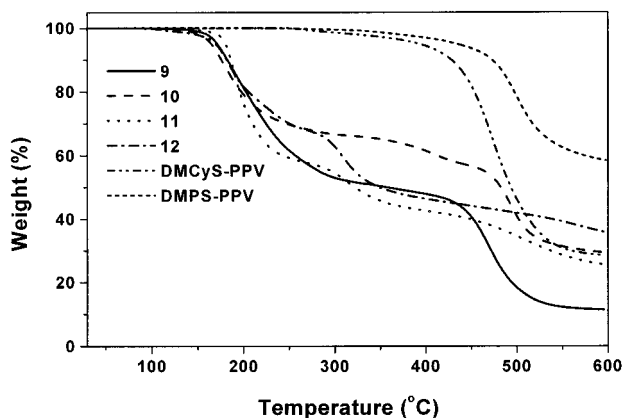


Figure 1. TGA thermograms of **9–12**, DMCyS-PPV, and DMPS-PPV.

PPV and DMPS-PPV also have improved mechanical properties, as measured by differential scanning calorimetry (DSC) measurements under a nitrogen atmosphere. The DSC curves show glass transition temperatures (T_g) of around 125 °C for DMCyS-PPV and 127 °C for DMPS-PPV. These values are high compared to those of the well-known alkoxy-substituted MEH-PPV (65 °C)²⁸ and are even comparable to those of polyfluorene derivatives (75–125 °C).^{29,30} This indicates that the incorporation of cyclohexylsilyl or phenylsilyl groups into the polymer side chain considerably suppresses the flexibility of the polymer and thus increases the T_g of the polymer. Recently, it was reported that the lifetime of EL devices is directly related to the T_g value and thermal stability of the polymers used.²⁰ Consequently, the good thermal stability and high T_g values of DMCyS-PPV and DMPS-PPV make them more suitable as EL polymers in terms of mechanical properties than simple alkylsilyl- or alkoxy-substituted PPVs. The polymerization results and thermal properties of all the polymers are summarized in Table 1.

Optical and Photoluminescence Properties. BDMCyS-PPV and BDMPS-PPV. The solid-state UV-vis absorption spectra of (a) BDMCyS-PPV and (b) BDMPS-PPV converted at various temperatures for 6 h in a vacuum are shown in Figure 2. Precursor polymers that have not been thermally treated do not show any absorption because they lack conjugation in the polymer main chain. On conversion at 100 °C, the absorption changes only a small amount, which suggests that only a small fraction of the precursor polymers was converted to the conjugated form at this temperature. However, polymer films converted at 150 °C in a vacuum show obvious changes in their absorption. This indicates that considerable H-Br elimination occurs at 150 °C, which is in accordance with the TGA analysis of the initial decomposition temperature of H-Br. Thin films containing BDMCyS-PPV and BDMPS-PPV with higher levels of conjugation were obtained from their respective precursor polymers by conversion at 200 and 250 °C than by treatment at lower temperatures. These polymers showed similar absorption profiles in terms of both the absorption maximum (413 nm for BDMCyS-PPV and 370 nm for BDMPS-PPV) and edge (493 nm for BDMCyS-PPV and 491 nm for BDMPS-PPV). The films treated at 300 °C for 6 h exhibited a diminished optical density and a slight blue shift in the absorption spectra (not shown here). These changes are due to the degradation of the conjugated polymer main chain. From these results we conclude that the onset of

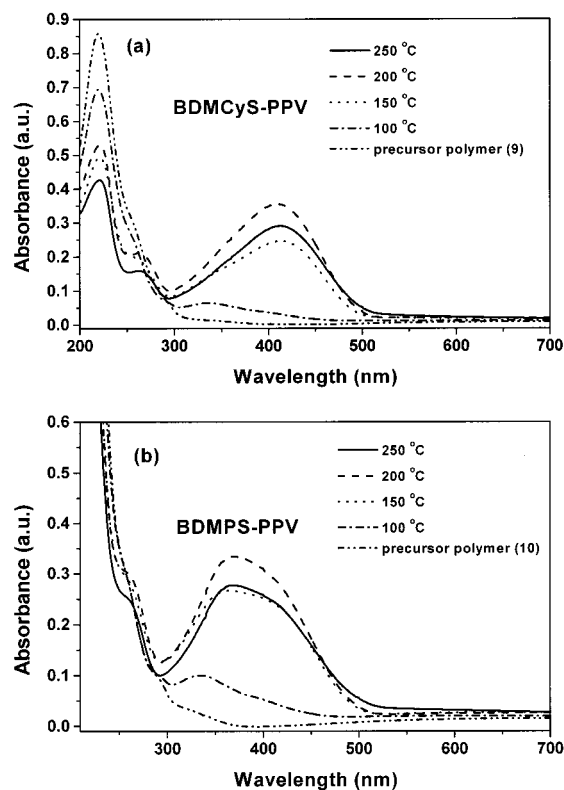


Figure 2. UV-vis absorption spectra of (a) BDMCyS-PPV and (b) BDMPS-PPV thin films thermally converted at the indicated temperatures for 6 h.

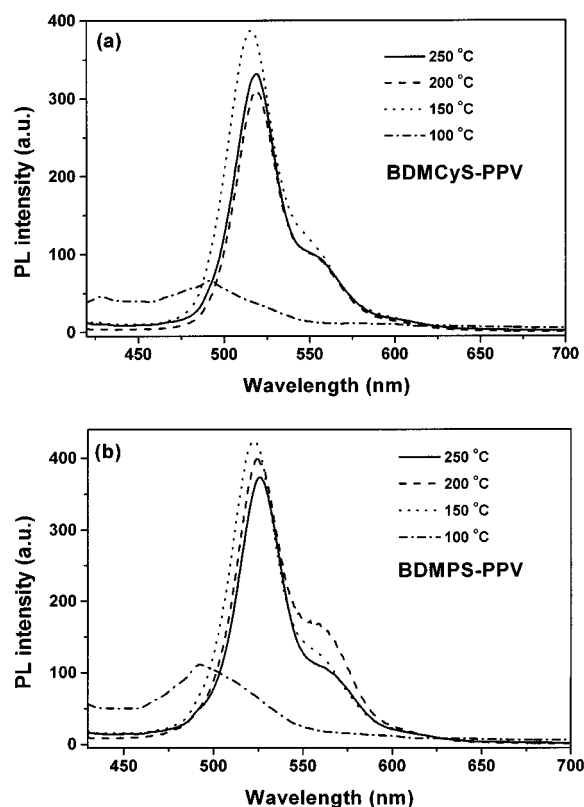


Figure 3. Photoluminescence (PL) spectra of (a) BDMCyS-PPV and (b) BDMPS-PPV thin films thermally converted at the indicated temperatures for 6 h.

conversion occurs at about 150 °C and fully conjugated polymers form at 250 °C. Figure 3 shows the solid-state photoluminescence (PL) spectra of (a) BDMCyS-PPV

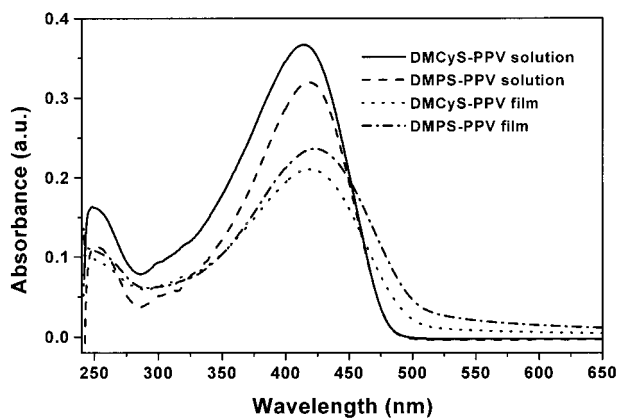


Figure 4. UV-vis absorption spectra of DMCyS-PPV and DMPS-PPV in solution and in thin films coated on a quartz plate.

and (b) BDMPS-PPV converted for 6 h in a vacuum at temperatures ranging from 100 to 250 °C. Only a small amount of emission is observed from the thin films maintained at 100 °C, indicating that the precursors are not converted at this temperature (as discussed above for the UV-vis absorption spectra). Above the onset conversion temperature (150 °C), however, greenish-yellow emissions appear. BDMCyS-PPVs converted at 200 and 250 °C show emission maxima at 519 nm with a shoulder at 555 nm, which are slightly red-shifted (4 nm) compared with those of the film converted at 150 °C. As with the absorption spectra, conversion above 300 °C leads to a blue shift in the emission and a significant decrease in emission intensity. Phenylsilyl-containing BDMPS-PPV converted at 250 °C shows a peak at 525 nm and a shoulder at 560 nm, corresponding to greenish-yellow emission.

DMCyS-PPV and DMPS-PPV. The final conjugated forms of the monosilyl-containing DMCyS-PPV and DMPS-PPV obtained by the Gilch method were completely soluble in common organic solvents. The UV-vis absorption spectra of these polymers both in dilute chloroform solutions and as thin films were measured and are shown in Figure 4. The maximum UV-vis absorptions of DMCyS-PPV and DMPS-PPV in solution appear at approximately 414 and 418 nm, respectively. The absorption maxima of the film samples were bathochromically red-shifted compared to the corresponding solution samples. The DMPS-PPV film shows a slight red shift of the absorption peak to 422 nm, whereas that of DMCyS-PPV shifts to 420 nm. This indicates that the π -electron delocalization of the polymer containing cyclohexylsilyl is interrupted to a greater extent than that in the polymer containing phenylsilyl.

Figure 5 shows the PL spectra recorded using excitation wavelengths corresponding to the absorption maximum of each polymer in solution and film. The PL spectra of DMCyS-PPV and DMPS-PPV in solution exhibit maximum emission peaks at 483 and 485 nm, respectively. The spectra of the film samples resemble those of the corresponding solutions but are shifted to longer wavelength. The DMCyS-PPV film shows a maximum emission peak at about 510 nm, with a shoulder at 545 nm. The phenylsilyl-substituted DMPS-PPV exhibits an almost the same emission profile similar to that of DMCyS-PPV, but with slightly red-shifted maximum emission and shoulder peaks at 513 and 547 nm, respectively. The reason for the red shift

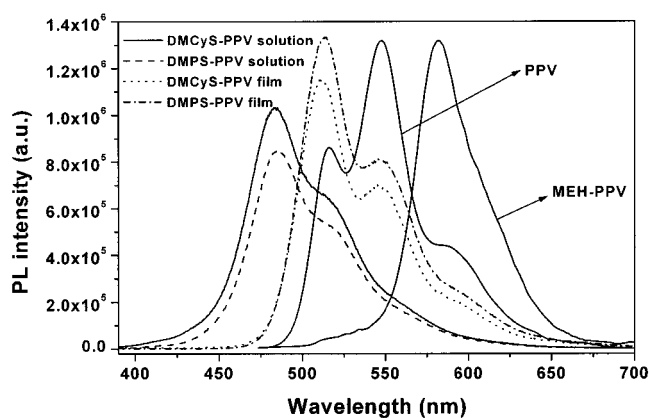


Figure 5. Photoluminescence (PL) spectra of DMCyS-PPV and DMPS-PPV in solution and in thin films coated on a quartz plate.

in the emission of DMPS-PPV compared with DMCyS-PPV is the same as that outlined above for the UV-vis absorption maxima of the two polymers. For comparison purposes, the PL spectra of the well-known PPV and alkoxy-substituted MEH-PPV are included in Figure 5. It can be seen that all the emission spectra of the silyl-substituted polymers are blue-shifted with respect to the PPV and MEH-PPV spectra. This blue shift results from the electronic properties of the silicon atoms, which have a slight electron-donating effect, and the greater steric hindrance of the bulky cyclohexylsilyl and phenylsilyl groups compared to other alkyl or alkoxy groups. These factors lead to a breaking of the coplanarity within the polymer main chain. Consequently, the cyclohexylsilyl or phenylsilyl substituents enlarge the semiconductor band through their blue-shifted emission compared with other PPV derivatives. Bis(silyl)-substituted BDMCyS-PPV and BDMPS-PPV show emissions that are slightly red-shifted with respect to DMCyS-PPV and DMPS-PPV; these results correlate with the symmetric structures of the bis(silyl)-substituted polymers ascertained from their low solubilities. Interestingly, the DMCyS-PPV and DMPS-PPV polymers are highly fluorescent in both solution and film. The quantum efficiency of each polymer in chloroform solution was determined twice more using a dilute quinine sulfate as a standard (ca. 1×10^{-5} M solution in 0.10 M H_2SO_4).^{31,32} The measured values were then averaged. The PL efficiency of quinine sulfate in 0.10 M H_2SO_4 solution was taken to be 0.546 at 365 nm excitation, and the refractive indices of the dilute polymer solutions in chloroform and 0.10 M H_2SO_4 were taken to be 1.446 and 1.333, respectively.¹⁹ Using these values, the quantum yields of DMCyS-PPV and DMPS-PPV were determined as $\Phi_{\text{sol}} = 0.88$ and 0.86, which are much higher than those of other PPVs containing alkoxy or alkyl side chains and are even comparable to those of polyfluorenes. In considering the utility of these compounds for applications in thin film displays, the film PL quantum efficiency is more meaningful than the solution value. The film PL efficiencies were measured using an optically dense configuration and diphenylanthracene (dispersed in a PMMA film at a concentration of less than 10^{-3} M, assuming a PL efficiency of 0.83) as the standard.^{29,32-34} DMCyS-PPV and DMPS-PPV showed extremely high film PL quantum efficiencies of $\Phi_{\text{film}} = 0.82$ and 0.83, respectively. These values are among the highest reported for the film PL efficiency of PPV derivatives. In our previous work in this area,

Table 2. UV-vis Spectra, Photoluminescence (PL) Spectra, and Quantum Yield in Solution and Film of Polymers

polymer	λ_{\max} (UV, nm) ^a		λ_{\max} (PL, nm) ^{a,b}		PL efficiency (Φ) ^a	
	soln	film	soln	film	soln	film
BDMCyS-PPV		413		519 (555)		0.53
BDMPS-PPV		370		525 (560)		0.56
DMCyS-PPV	414	420	483 (515)	510 (545)	0.88	0.82
DMPS-PPV	418	422	485 (517)	513 (547)	0.86	0.83

^a These values listed were measured in chloroform solution and thin film state onto the quartz plate. ^b These values listed in parentheses represent shoulder peak.

we reported a solid PL quantum efficiency of $\Phi_{\text{film}} = 0.81$ from the copolymer composed of alkyl-substituted fluorene and trimethylsilyl-substituted phenyl moieties.⁷ The polymers containing bis(silyl) obtained by thermal elimination at 250 °C, BDCyS-PPV ($\Phi_{\text{film}} = 0.53$) and BDMPS-PPV ($\Phi_{\text{film}} = 0.56$), exhibited lower film PL efficiencies than the mono-Si-substituted DMCyS-PPV and DMPS-PPV. It seems that the better packing of the polymers with symmetric cyclohexylsilyl or phenylsilyl side chains reduces the quantum efficiency. In other words, the chain packing and conjugation are more effectively interrupted in the monosilyl-substituted systems (DMCyS-PPV and DMPS-PPV) than the bis(silyl)-substituted symmetric ones (BDMCyS-PPV and BDMPS-PPV), which results in the formation of amorphous polymer thin films for an increased luminescence. The absorption and photoluminescence results for the cyclohexylsilyl- and phenylsilyl-substituted PPVs in solution and film states are summarized in Table 2.

Electrochemical Properties. Cyclic voltammetry (CV) is an easy and effective approach for measuring redox reversibility, reproducibility, and stability of polymer films on electrodes. In addition, it can be utilized to simultaneously evaluate both the HOMO and LUMO energy levels and the band gap of a polymer. CV was performed on a solution of 0.1 M tetrabutylammonium tetrafluoroborate (Bu_4NBF_4) in acetonitrile with a scan rate of 50 mV/s at room temperature under the protection of argon. A platinum electrode ($\sim 0.5 \text{ cm}^2$) was coated with a thin polymer film (DMCyS-PPV or DMPS-PPV) and used as the working electrode. Platinum wire was used as the counter electrode, and a Ag/0.10 M AgNO_3 electrode was used as the reference electrode. The cyclic voltammograms from DMCyS-PPV, DMPS-PPV, and MEH-PPV are displayed in Figure 6. During the cathodic scan, DMPS-PPV exhibits reversible n-doping processes. $E_{\text{pc/pa}}$ were found at $-1.89/-1.68 \text{ V}$ vs SCE, and the onset of the n-doping process occurs at about -1.75 V . DMCyS-PPV showed similar peaks and onset potentials in the n-doping process, but with a slightly lower onset potential (-1.81 V) than DMPS-PPV for reduction. This indicates that DMCyS-PPV has a lower electron affinity than DMPS-PPV for accepting electrons from the cathode in an EL device. In the anodic scan, DMCyS-PPV and DMPS-PPV show similar irreversible p-doping processes. DMCyS-PPV and DMPS-PPV exhibit peak potentials at 1.47 and 1.27 V, respectively. The onset potential of oxidation for DMCyS-PPV (1.25 V) is somewhat higher than the value for DMPS-PPV (1.16 V). For comparison, we also measured the electrochemical properties of the well-known polymer MEH-PPV. The cyclic voltammogram of MEH-PPV measured in the present

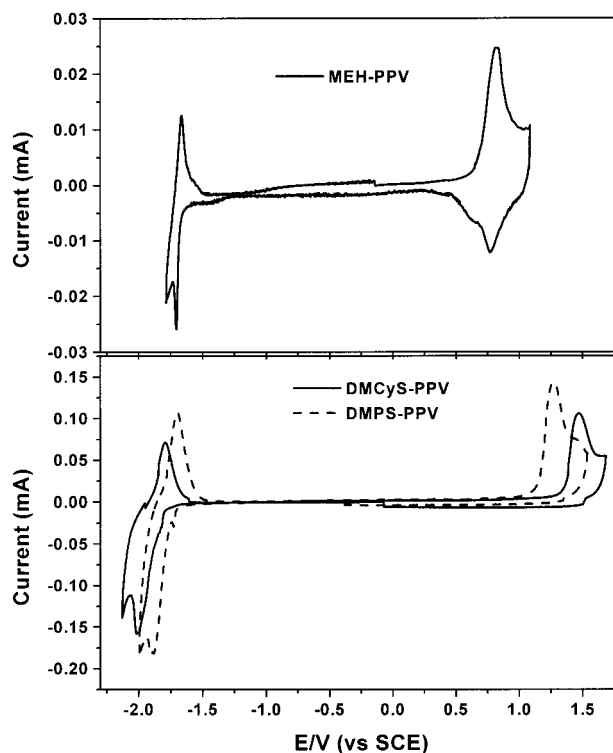


Figure 6. Cyclic voltammograms of MEH-PPV, DMCyS-PPV, and DMPS-PPV films coated on platinum plate electrode in acetonitrile containing 0.1 M Bu_4NBF_4 . Counter electrode: platinum wire. Reference electrode: Ag/AgNO₃ (0.1 M in acetonitrile). Scan rate: 50 mV/s.

study coincides well with previous results.³⁵ Compared to MEH-PPV, DMCyS-PPV and DMPS-PPV show much lower peak currents in the cathodic reaction. This result indicates that polymers with cyclohexylsilyl or phenylsilyl in PPV backbone have a greater potential for accepting or transporting electrons than alkoxy-substituted PPV derivatives (e.g., MEH-PPV). The onset potentials (E_{ox} and E_{red}) of p- and n-doping are used to determine the HOMO and LUMO energy levels of the conjugated polymers by means of the empirical relationship proposed by Leeuw et al.³⁶ This relationship connects the solid-state IP (HOMO) and EA (LUMO) to the E_{ox} and E_{red} using the relations $\text{IP} (E_{\text{HOMO}}) = -(E_{\text{ox}} + 4.39) \text{ (eV)}$ and $\text{EA} (E_{\text{LUMO}}) = -(E_{\text{red}} + 4.39) \text{ (eV)}$, where E_{HOMO} is the HOMO energy level and E_{LUMO} is the LUMO energy level below the vacuum. These data are useful for the selection of suitable electrode materials and hole- or electron-transporting materials in the fabrication of effectively balanced polymer EL devices. All the data, including the IP (E_{HOMO}) and EA (E_{LUMO}) values, electrochemical band gaps, oxidation and reduction onset potentials, and n-doping and p-doping peak potentials, are listed in Table 3. As shown in Table 3, DMCyS-PPV has a more negative value of IP (HOMO) than DMPS-PPV. The cyclohexylsilyl- and phenylsilyl-substituted polymers have much more negative [IP (HOMO)] values than other PPV derivatives. This property means that it is difficult to inject holes from indium tin oxide (ITO) into the polymers. Similar results are reported elsewhere for other simple alkylsilyl-substituted polymers.¹⁹ Alkyl- or alkoxy-substituted PPV derivatives usually have hole major characteristics in EL devices, imbalance of injected hole and electron, with an air-stable metal cathode.³⁷ However, DMCyS-PPV and DMPS-PPV with retarded hole injection show

Table 3. Electrochemical Properties and Energy Levels of MEH-PPV, DMCyS-PPV, and DMPS-PPV

polymer	n-doping (V) ^a			p-doping (V) ^a			energy levels (eV)		
	E_{onset}	E_{pa}	E_{pc}	E_{onset}	E_{pa}	E_{pc}	IP	EA	band gap
DMCyS-PPV	-1.81	-1.77	-2.01	1.25	1.47		-5.64	-2.58	3.06
DMPS-PPV	-1.75	-1.68	-1.89	1.16	1.27		-5.55	-2.64	2.91
MEH-PPV	-1.57	-1.66	-1.70	0.55	0.82	0.77	-4.94	-2.82	2.12

^a E_{onset} , E_{pa} , and E_{pc} stand for onset potential, anodic peak potential, and cathodic peak potential, respectively.

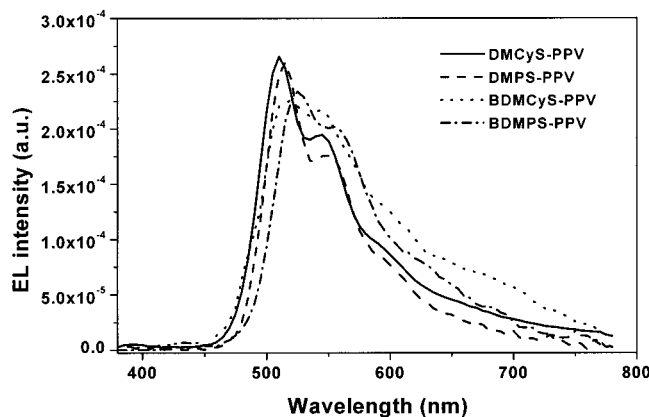


Figure 7. Electroluminescence (EL) spectra of single-layer LEDs of BDMCyS-PPV, BDMPS-PPV, DMCyS-PPV, and DMPS-PPV with a configuration of ITO/polymer/Al.

more balanced hole and electron injection than PPV derivatives, allowing the construction of an improved EL device with an air-stable cathode.

Electroluminescent Device Characteristics. BDMCyS-PPV and BDMPS-PPV. Single-layer EL devices were fabricated from polymer films sandwiched between ITO anodes and aluminum cathodes. Precursor polymer solutions were spin-coated onto ITO and then thermally converted to give the conjugated polymers. Aluminum electrodes were then evaporated onto the top of the polymer film to complete the devices. Electroluminescence (EL) was observed from both polymer devices; the spectra are shown in Figure 7. The EL emission maxima from the ITO/BDMCyS-PPV/Al and ITO/BDMPS-PPV/Al devices are at 518 and 525 nm, respectively. As a consequence, emission from these devices appears greenish-yellow to the eye. In addition, the devices show similar vibronic emissions at about 542 nm (BDMCyS-PPV) and 556 nm (BDMPS-PPV), as in the PL spectra. The luminance of the ITO/BDMCyS-PPV/Al device was rather low, reaching only 6 cd/m² at 15 V, 90 mA/cm². BDMPS-PPV showed a higher maximum luminance (11 cd/m² at 14 V, 165 mA/cm²) than BDMCyS-PPV in the device of structure ITO/polymer/Al. The threshold voltages of BDMCyS-PPV and BDMPS-PPV polymers were about 8 and 9 V (film thickness approximately 100 nm), respectively. Consequently, EL devices consisting of BDMCyS-PPV or BDMPS-PPV films fabricated by thermal conversion exhibited rather low performance compared with other silyl-substituted PPVs. We believe that these results have the same origin as the PL efficiency results outlined above; namely, the polymer chain packing of symmetric structures decreases the efficiency of PL and EL. Nevertheless, the thermally converted BDMCyS-PPV and BDMPS-PPV films do not dissolve or swell in common organic solvents. This solubility behavior can be applied advantageously in the design of multilayer polymer LED devices.³

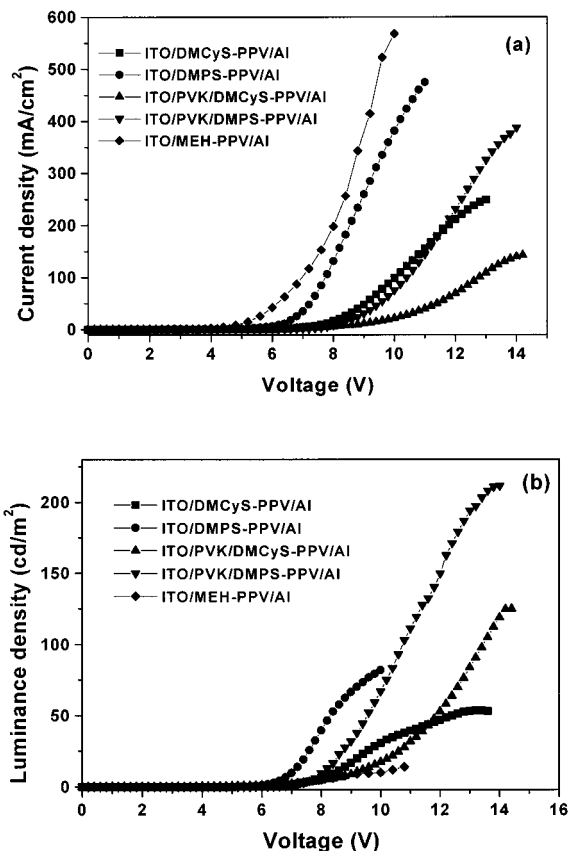


Figure 8. (a) Current-voltage or (b) luminance-voltage characteristics of single- and double-layer LEDs of MEH-PPV, DMCyS-PPV, and DMPS-PPV with a configuration of ITO/polymer/Al and ITO/PVK/polymer/Al.

DMCyS-PPV and DMPS-PPV. The EL spectra of DMCyS-PPV and DMPS-PPV from the device configuration ITO/polymer/Al are shown in Figure 7. DMCyS-PPV and DMPS-PPV exhibit EL emissive bands at 510 and 515 nm, respectively. These emissions correspond to green light, which represents a slight blue shift with respect to the bis(silyl) systems BDMCyS-PPV and BDMPS-PPV. Figure 8 shows (a) current-voltage and (b) luminance density-voltage characteristics of the ITO/polymer/Al and ITO/PVK/polymer/Al devices. The characteristics of the well-known dialkoxy-substituted MEH-PPV were also determined to compare device performance. All polymer films were about 80 nm in thickness. DMCyS-PPV and DMPS-PPV showed good device performance in single-layer EL devices with air-stable Al electrodes compared with BDMCyS-PPV, BDMPS-PPV, and MEH-PPV. DMCyS-PPV and DMPS-PPV showed maximum luminance values of about 54 and 91 cd/m² at 11 and 13 V, respectively. The external quantum efficiency and power efficiency of DMPS-PPV reached 0.025% and 0.047 lm/W, which are much higher than those of MEH-PPV (measured at about $2 \times 10^{-3}\%$ external efficiency).³⁸ Moreover, DMCyS-PPV and DMPS-PPV

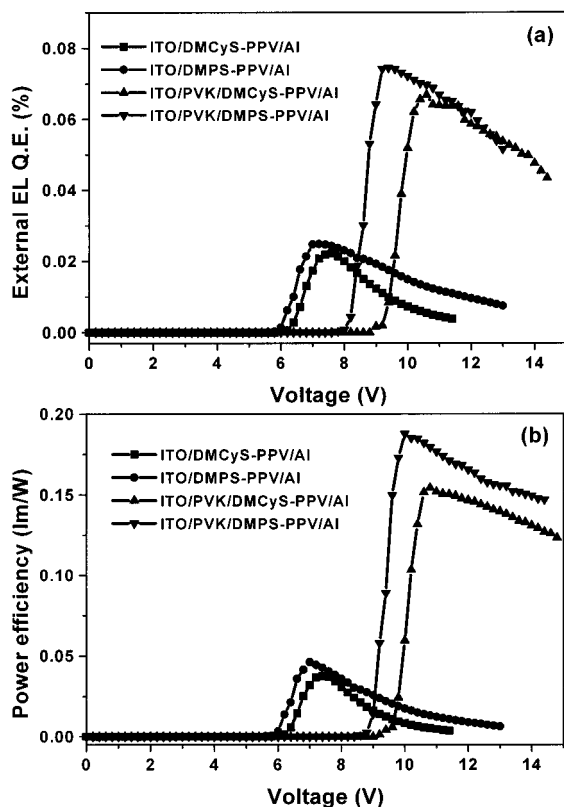


Figure 9. (a) External quantum efficiency and (b) power efficiency of single- or double-layer light-emitting diodes of DMCyS-PPV and DMPS-PPV.

showed lower turn-on voltages (7 and 6 V, respectively) than octylsilyl-substituted DMOS-PPV (> 10 V)¹⁷ and comparable turn-on voltages to those measured for simple alkylsilyl-substituted PPVs in a single-layer EL device with a Mg:Ag cathode.¹⁹ The bilayer devices with an ITO/PVK/polymer/Al structure showed drastically improved luminance values. Compared with alkyl- or alkoxy-PPVs, DMCyS-PPV and DMPS-PPV have higher energy barriers (from CV data) between ITO and the HOMO of the polymers. To reduce the effect of this barrier, we inserted a layer of PVK (5.4 eV) between the ITO (4.8 eV) and polymer layers (DMCyS-PPV (5.64 eV) and DMPS-PPV (5.55 eV)) to facilitate hole transportation. Figure 8 shows that the turn-on voltages of the double-layer devices are about 2–3 V higher than those of the single-layer devices, but the DMCyS-PPV and DMPS-PPV double-layer devices containing PVK exhibit much higher values of the maximum brightness, external quantum efficiency, and power efficiency. The ITO/PVK/DMPS-PPV/Al device reached a maximum brightness of about 220 cd/m² at 14 V and showed 0.075% and 0.187 lm/W for the external quantum efficiency and power efficiency, respectively. The EL spectra of these devices are the same as those of the single-layer devices, presented in Figure 7. The external quantum efficiency and power efficiency curves of the single- and double-layer EL devices of DMCyS-PPV and DMPS-PPV are shown in Figure 9. To improve the performance of the EL device, a PEDOT:PSS layer of thickness 30 nm was inserted between the ITO and the PVK layer, and an LiF layer of thickness 2 nm was inserted between the DMPS-PPV and Al. PEDOT:PSS is widely used as a hole injection layer, and the thin LiF layer acts as an insulating layer that decreases the barrier to electron injection from the cathode (Al) to the

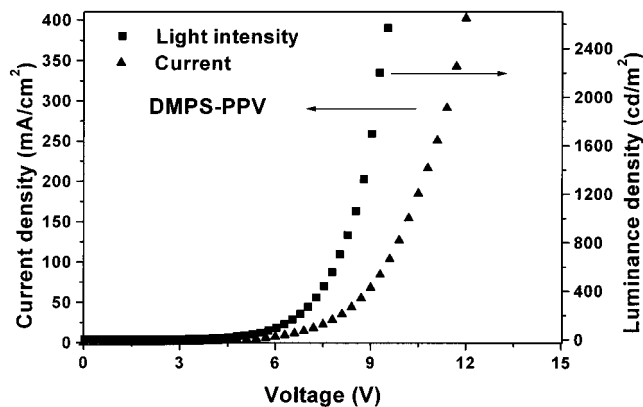


Figure 10. Current–luminance–voltage (I – V – L) characteristics for an ITO/PEDOT:PSS (30 nm)/PVK (60 nm)/DMPS-PPV (80 nm)/LiF (2 nm)/Al.

polymer LUMO.^{39–41} Figure 10 shows that maximum brightness of this multilayer device is 2450 cd/m² at 370 mA/cm² (12 V), with a turn-on voltage of 5 V. This value is much higher than the currently reported value (1384 cd/m² at 12 V) of alkoxy- and bis(silyl)-substituted BDMPS-*co*-DB-PPV in a similar EL device configuration (ITO/PEDOT/polymer/Ca), which differs only in the lack of the PVK layer used in our device.⁴²

Conclusions

We have reported the synthesis of novel cyclohexylsilyl- or phenylsilyl-substituted PPVs using the bromine precursor route (BPR) to prepare bis(silyl)-substituted polymers and Gilch polymerization to prepare monosilyl-substituted polymers. We successfully fabricated insoluble BDMCyS-PPV and BDMPS-PPV thin films from precursor polymers by thermal conversion. These insoluble films are suitable for applications in multilayer polymer EL devices. The monosilyl systems containing cyclohexyl or phenyl were shown to be superior to the bis(silyl) systems in solubility (processability), film PL efficiency, and EL efficiency. The monosilyl-substituted polymers DMCyS-PPV and DMPS-PPV showed higher T_g , molecular weight, and thermal stability than the alkoxy or simple alkylsilyl-PPVs. In addition, DMCyS-PPV and DMPS-PPV exhibited very high solution and film PL efficiencies combined with good processability, amorphousness, and good film-forming ability. Overall, cyclohexylsilyl- or phenylsilyl substituents have much better properties than other substituents such as alkoxy or alkyl groups. The single and double-layer EL devices of DMCyS-PPV and DMPS-PPV using air-stable aluminum cathodes emitted green light with good brightness and efficiency. Addition of a thin PEDOT:PSS layer and a dielectric LiF layer led to an improved maximum luminance of 2450 cd/m² at 370 mA/cm² (12 V) and a turn-on voltage of 5 V. The characteristics of DMCyS-PPV and DMPS-PPV such as good thermal stability and luminance properties make them potential candidates for application in polymer LEDs.

Acknowledgment. This work was supported by the Center for Advanced Functional Polymers through the Korea Science and Engineering Foundation (KOSEF) and ILJIN. The authors are grateful to Dr. Jeong-Ik Lee at ETRI for helpful experiments and discussions on the EL device fabrication and measuring the I – V – L characteristics. This paper is dedicated to Professor Jung-Il Jin on the occasion of his 60th birthday.

References and Notes

- (1) Burroughes, J. H.; Bradley, D. D. C.; Brown, A. R.; Marks, R. N.; Mackay, K.; Friend, R. H.; Burns, P. L.; Holmes, A. B. *Nature (London)* **1990**, *347*, 539.
- (2) Braun, D.; Heeger, A. J. *Appl. Phys. Lett.* **1991**, *58*, 1982.
- (3) Kraft, A.; Grimsdale, A. C.; Holmes, A. B. *Angew. Chem., Int. Ed.* **1998**, *37*, 402.
- (4) Friend, R. H.; Gymer, R. W.; Holmes, A. B.; Burroughes, J. H.; Marks, R. N.; Taliani, C.; Bradley, D. D. C.; dos Santos, D. A.; Bredas, J. L.; Logdlund, M.; Salaneck, W. R. *Nature (London)* **1999**, *397*, 121.
- (5) Gustafsson, G.; Cao, Y.; Treacy, G. M.; Klavetter, F.; Colaneri, N.; Heeger, A. J. *Nature (London)* **1992**, *357*, 477.
- (6) Greenham, N. C.; Moratti, S. C.; Bradley, D. D. C.; Friend, R. H.; Holmes, A. B. *Nature (London)* **1993**, *365*, 628.
- (7) (a) Ahn, T.; Jang, M. S.; Shim, H. K.; Hwang, D. H.; Zyung, T. *Macromolecules* **1999**, *32*, 3279. (b) Ahn, T.; Song, S. Y.; Shim, H. K. *Macromolecules* **2000**, *33*, 6764.
- (8) Grem, G.; Leditzky, G.; Ullrich, B.; Leising, G. *Adv. Mater.* **1992**, *4*, 36.
- (9) Grem, G.; Leditzky, G.; Ullrich, B.; Leising, G. *Synth. Met.* **1992**, *51*, 383.
- (10) Andersson, M. R.; Thomas, O.; Mammo, W.; Svensson, M.; Theander, M.; Inganäs, O. *J. Mater. Chem.* **1999**, *9*, 1933.
- (11) Fukuda, M.; Sawada, K.; Yoshino, K. *Jpn. J. Appl. Phys.* **1989**, *28*, L1433.
- (12) Pei, Q.; Yang, Y. *J. Am. Chem. Soc.* **1996**, *118*, 7416.
- (13) Miller, R. D.; Klaerner, G. *Macromolecules* **1998**, *31*, 2007.
- (14) Spreitzer, H.; Becker, H.; Kluge, E.; Kreuder, W.; Schenk, H.; Demandt, R.; Schöo, H. *Adv. Mater.* **1998**, *10*, 1340.
- (15) Höger, S.; McNamara, J. J.; Schrickler, S.; Wudl, F. *Chem. Mater.* **1994**, *6*, 171.
- (16) Zhang, C.; Höger, S.; Pakabaz, K.; Wudl, F.; Heeger, A. J. *J. Electron. Mater.* **1994**, *23*, 453.
- (17) Hwang, D. H.; Kim, S. T.; Shim, H. K.; Holmes, A. B.; Moratti, S. C.; Friend, R. H. *Chem. Commun.* **1996**, 2241.
- (18) Kim, S. T.; Hwang, D. H.; Li, X. C.; Gruner, J.; Friend, R. H.; Holmes, A. B.; Shim, H. K. *Adv. Mater.* **1996**, *8*, 979.
- (19) Chen, Z.-K.; Huang, W.; Wang, L.-H.; Kang, E.-T.; Chen, B. J.; Lee, C. S.; Lee, S. T. *Macromolecules* **2000**, *33*, 9015.
- (20) Tokito, S.; Tanaka, H.; Noda, K.; Okada, A.; Taga, Y. *Appl. Phys. Lett.* **1997**, *70*, 1929.
- (21) Wan, W. C.; Antoniadis, H.; Choong, V. E.; Razafitrimo, H.; Gao, Y.; Feld, W. A.; Hsieh, B. R. *Macromolecules* **1997**, *30*, 6567.
- (22) Hsieh, B. R.; Wan, W. C.; Yu, Y.; Gao, Y.; Goodwin, T. E.; Gonzalez, S. A.; Feld, W. A. *Macromolecules* **1998**, *31*, 631.
- (23) Boardman, F. H.; Grice, A. W.; Rütther, M. G.; Sheldon, T. J.; Bradley, D. D. C.; Burn, P. L. *Macromolecules* **1999**, *32*, 111.
- (24) Gilch, H. G.; Wheelwright, W. L. *J. Polym. Sci., Part A-1: Polym. Chem.* **1966**, *4*, 1337.
- (25) Becker, H.; Spreitzer, H.; Ibrom, K.; Kreuder, W. *Macromolecules* **1999**, *32*, 4925.
- (26) Wudl, F.; Allemand, P. M.; Srdanov, G.; McBranch, Z. Ni, D. *ACS Symp. Ser.* **1991**, *455*. Wudl, F. (University of California), US-B 5 189 136, 1990 [*Chem. Abstr.* **1993**, *118*, 255575p].
- (27) Heeger, A. J.; Braun, D. (UNIAX), WO-B 92/16023, 1992 [*Chem. Abstr.* **1993**, *118*, 157401j].
- (28) Liu, Y.; Liu, M. S.; Li, X.-C.; Jen, A. K.-Y. *Chem. Mater.* **1998**, *10*, 3301.
- (29) Kreyenschmidt, M.; Klaerner, G.; Fuher, T.; Ashenhurst, J.; Karg, S.; Chen, W. D.; Lee, V. Y.; Scott, J. C.; Miller, R. D. *Macromolecules* **1998**, *31*, 1099.
- (30) Zheng, L.; Urian, R. C.; Liu, Y.; Jen, A. K.-Y.; Pu, L. *Chem. Mater.* **2000**, *12*, 13.
- (31) Joshi, H. S.; Jamshidi, R.; Tor, Y. *Angew. Chem., Int. Ed.* **1999**, *38*, 2722.
- (32) Demas, J. N.; Crosby, G. A. *J. Phys. Chem.* **1971**, *75*, 991.
- (33) Guilbaut, G. G., Ed.; *Practical Fluorescence*, 2nd ed.; Marcel Dekker Inc.: New York, 1990.
- (34) Pang, Y.; Li, J.; Hu, B.; Karasz, F. E. *Macromolecules* **1998**, *31*, 6730.
- (35) Meng, H.; Yu, W. L.; Huang, W. *Macromolecules* **1999**, *32*, 8841.
- (36) Leeuw, D. M.; Simenon, M. M. J.; Brown, A. R.; Einerhand, R. E. F. *Synth. Met.* **1997**, *87*, 53.
- (37) Parker, I. D. *J. Appl. Phys.* **1994**, *75*, 1656.
- (38) Cao, Y.; Yu, G.; Heeger, A. J. *Adv. Mater.* **1998**, *10*, 917.
- (39) Groenendaal, L.; Jonas, F.; Freitag, D.; Pielartzik, H.; Reynolds, J. R. *Adv. Mater.* **2000**, *12*, 481.
- (40) Hung, L. S.; Tang, C. W.; Mason, M. G. *Appl. Phys. Lett.* **1997**, *70*, 152.
- (41) Wakimoto, T.; Fukuda, Y.; Nakayama, K.; Yokoi, A.; Nakada, H.; Tsuchida, M. *IEEE Trans. Electron Devices* **1997**, *44*, 1245.
- (42) Martin, R. E.; Geneste, F.; Riehn, R.; Chuah, B. S.; Cacialli, F.; Friend, R. H.; Holmes, A. B. *Chem. Commun.* **2000**, 291.

MA011618B